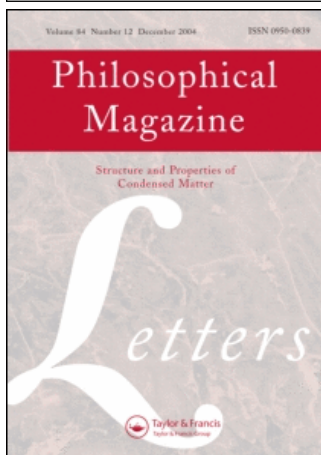


This article was downloaded by:[University of California Berkeley]
On: 1 October 2007
Access Details: [subscription number 769844257]
Publisher: Taylor & Francis
Informa Ltd Registered in England and Wales Registered Number: 1072954
Registered office: Mortimer House, 37-41 Mortimer Street, London W1T 3JH, UK



Philosophical Magazine Letters

Publication details, including instructions for authors and subscription information:
<http://www.informaworld.com/smpp/title~content=t713695410>

Magnetoelectric complex-oxide heterostructures

R. Ramesh^a; F. Zavaliche^a; Y. H. Chu^a; L. W. Martin^a; S. Y. Yang^a; M. P. Cruz^a; M. Barry^a; K. Lee^a; P. Yang^a; Q. Zhan^a

^a Department of Materials Science and Engineering, and Department of Physics, University of California, Berkeley, CA 94720, USA

Online Publication Date: 01 March 2007

To cite this Article: Ramesh, R., Zavaliche, F., Chu, Y. H., Martin, L. W., Yang, S. Y., Cruz, M. P., Barry, M., Lee, K., Yang, P. and Zhan, Q. (2007) 'Magnetoelectric complex-oxide heterostructures', *Philosophical Magazine Letters*, 87:3, 155 - 164

To link to this article: DOI: 10.1080/09500830701235786

URL: <http://dx.doi.org/10.1080/09500830701235786>

PLEASE SCROLL DOWN FOR ARTICLE

Full terms and conditions of use: <http://www.informaworld.com/terms-and-conditions-of-access.pdf>

This article maybe used for research, teaching and private study purposes. Any substantial or systematic reproduction, re-distribution, re-selling, loan or sub-licensing, systematic supply or distribution in any form to anyone is expressly forbidden.

The publisher does not give any warranty express or implied or make any representation that the contents will be complete or accurate or up to date. The accuracy of any instructions, formulae and drug doses should be independently verified with primary sources. The publisher shall not be liable for any loss, actions, claims, proceedings, demand or costs or damages whatsoever or howsoever caused arising directly or indirectly in connection with or arising out of the use of this material.

Magnetoelectric complex-oxide heterostructures

R. RAMESH*, F. ZAVALICHE, Y. H. CHU,
L. W. MARTIN, S. Y. YANG, M. P. CRUZ, M. BARRY,
K. LEE, P. YANG and Q. ZHAN

Department of Materials Science and Engineering,
and Department of Physics, University of California,
Berkeley, CA 94720, USA

(Received 18 December 2006; in final form 10 January 2007)

A short review of recent progress in the field of multiferroic thin films and heterostructures is given. We focus on the bismuth iron oxide system due to its desirable properties, namely high ferroelectric Curie temperature and antiferromagnetic Neel temperature. Epitaxial growth of this model system in various crystallographic orientations has conclusively demonstrated the large ferroelectric polarization in this system. Piezoforce microscopy reveal a complex domain structure, especially on (100) SrTiO₃ substrates. Electrical switching experiments show the co-existence of 71°, 109° and 180° domain switching mechanisms in such films. Preliminary work has shown promise for electrically controllable exchange bias in ferromagnet–multiferroic heterostructures.

1. Introduction

Materials which exhibit simultaneous magnetic and ferroelectric ordering, ferro-electro-magnets in short, have been the focus of research for decades due to their fascinating materials physics and emergent technological potential [1]. Coupling between the corresponding order parameters was theoretically predicted previously [2] and is currently a topic of intense interest [3–5]. However, single phase materials, which simultaneously show high magnetization and polarization at ambient conditions, remain elusive [6]. Therefore, studies of such materials, e.g. manganites, have only been performed at low temperatures [7–9]. An alternative approach uses bonded magnetic and piezoelectric layers to investigate the room temperature magnetoelectric coupling at macroscopic scales [10, 11].

The whole field of multiferroics [3–5] has been rejuvenated by the recent reports on large room temperature ferroelectric polarization and strong piezoelectric response in epitaxial BiFeO₃ (BFO) films [12–16]. This was in sharp contrast to the weak polarization observed earlier on bulk ceramics [17], but in very good agreement with the theoretical results [18–21]. Very recently, large polarization values have been reported in bulk single crystals as well [22]. This material simultaneously shows antiferromagnetic and ferroelectric order with the

*Corresponding author. Email: rramesh@berkeley.edu

corresponding transition temperatures well above room temperature, i.e. $T_N \sim 370^\circ\text{C}$ and $T_C \sim 830^\circ\text{C}$, respectively [23]. Therefore, questions have arisen as to whether the corresponding order parameters couple to each other [12, 18, 19, 24], as in the case of e.g. BaFMn_4 [25–28] and some multiferroic manganites [7–9] with low transition temperatures. It was not until very recently that the coupling between the antiferromagnetic and ferroelectric order in epitaxial BiFeO_3 films has been explored [29]. Moreover, the possibility of growing high quality epitaxial BiFeO_3 thin films has also enabled the observation of weak magnetism [12, 30, 31], but its origin is not yet fully established [32, 33].

The structure of BiFeO_3 (sketched in figure 1) is characterized by two distorted perovskite blocks ($a_r = 3.96 \text{ \AA}$, $\alpha_r = 0.6^\circ$) connected along their body diagonal (figure 1a), denoted as pseudocubic $\langle 111 \rangle$, to build the rhombohedral unit cell [34, 35]. The ferroelectric state is realized by a large displacement of the Bi ions relative to the FeO_6 octahedra (figure 1b). Two important consequences result from this atomic arrangement. First, polarization lies along the $\langle 111 \rangle$, leading to the formation of eight possible polarization variants ($P_i^{+/-}$ with $i = \{1, 2, 3, 4\}$; ‘+’ and ‘-’ indicate for up and down polarization directions, respectively). These eight polarization directions correspond to four structural variants [14, 35–39]. Second, Fe magnetic moments couple ferromagnetically within the pseudocubic $\{111\}$ planes and antiferromagnetically between adjacent planes [18]. Since the coupling between ferroelectricity and magnetism in BiFeO_3 is determined by rotations of the oxygen octahedral [18], 71° ($P_i^{+/-}$ to $P_{i\pm 2}^{-/+}$) and 109° ($P_i^{+/-}$ to $P_{i\pm 1}^{-/+}$) rotations of polarization from one $\langle 111 \rangle$ axis to the other three $\langle 111 \rangle$ axes, rather than 180° switching along the same $\langle 111 \rangle$ axis ($P_i^{+/-}$ to $P_i^{-/+}$), might lead to changes in the magnetic

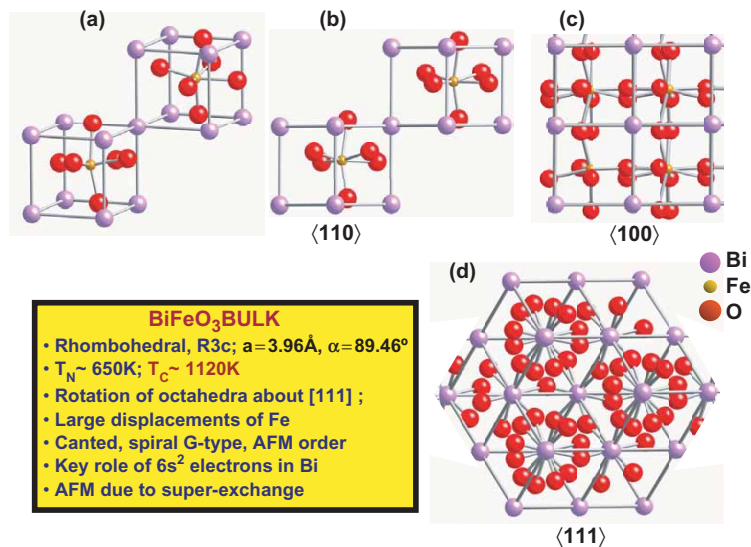


Figure 1. Structure of rhombohedral BiFeO_3 viewed along different crystallographic directions and a summary of its physical properties.

ultrathin epitaxial films on (001) STO show a strong tetragonal distortion superimposed on the rhombohedral crystal structure, leading to a monoclinic symmetry at such thicknesses. There has been a strong focus on (001) STO substrates, since they are reasonably well lattice-matched and are also more readily available. The ferroelectric domain structure of films in this orientation appears to be quite sensitive to substrate miscut angles, growth mechanisms (which in turn is controlled by the deposition rate) and the quality of the SRO layer underneath.

3. Ferroelectric properties

In the early days of research on this system, the ferroelectric properties of the BiFeO₃ system were initially under intense scrutiny, especially since previous reports on bulk and single crystals had indicated a rather low spontaneous polarization. Over the past several years, however, it has become clear that BiFeO₃ indeed has a large spontaneous and switchable polarization. Using substrates of various orientations [(001), (110) and (111)] (figure 3), we have been able to clearly demonstrate that the spontaneous polarization is indeed along the $\langle 111 \rangle$ direction with a magnitude of 90–95 $\mu\text{C}/\text{cm}^2$, consistent with first principles calculations. Several aspects of this data are noteworthy. First, the coercive field is significantly higher than the corresponding values for the Pb(Zr_xTi_{1-x}O₃) system (PZT). For FeRAM applications, a value 50–70 kV/cm would be desirable (translating to a coercive voltage of 0.5–0.7V for a 100-nm thick film). Second, the coercive field is higher in the (111) orientation compared to the (100)-oriented film. The origin of this difference is not clear, although it is likely that this can be traced back to the domain structure

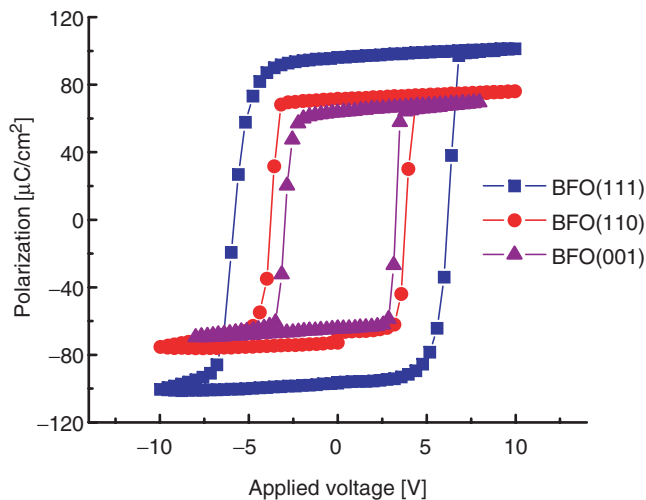


Figure 3. Ferroelectric polarization loops measured on epitaxial BiFeO₃ films with different crystallographic orientations.

and their dynamics. Therefore, over the past couple of years, we have been spending a significant amount of effort on understanding the domain structure as a function of substrate orientation, film growth conditions and how these domains influence the ferroelectric switching properties.

4. Domain structure and dynamics

In the following, we present the main results on domain structure in (001)-oriented epitaxial BiFeO_3 films. We will then discuss the possible electrical bias-induced polarization switching mechanisms as deduced from the changes in domain pattern. The domain structure in rhombohedral ferroelectrics on a 001-type cubic surface can be rather complicated [14, 37] due to the possible coexistence of eight polarization variants [35, 36, 39]. In PFM, domains with up (P_i^+) and down (P_i^-) polarizations give rise to opposite contrast in out-of-plane (OP) PFM (black and white, respectively). Domains with polarization vectors along the cantilever's long axis do not give rise to in-plane (IP) PFM signal (zero amplitude) for they do not produce any torque required for IP imaging [45]. Instrumental offsets often make these domains appear with a non-zero piezo-response (PR) signal. Also, domains with polarization pointing to the right with respect to the cantilever's long axis should produce an opposite tone as compared with domains having polarization pointing to the left, due to the antiphase IP-PR signals produced by these domains.

We analyze the amplitude, phase and in-phase PFM images taken along a $\langle 110 \rangle$ direction on a 600-nm thick BiFeO_3 (001) film, which exhibits a stripe domain pattern with two polarization variants [15]. The information provided by amplitude images (figure 4a, b) contains the magnitude of PR. These images show two tones,

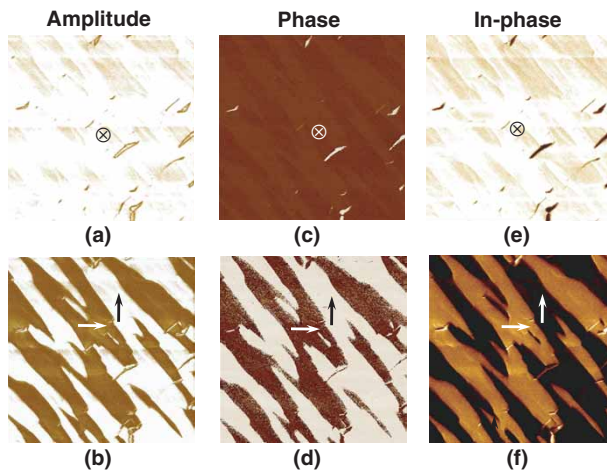


Figure 4. Stripe domain pattern of an epitaxial BiFeO_3 film imaged by PFM. (a), (c), (e) Out-of-plane and (b), (d), (f) in-plane PFM scans: (a), (b) amplitude, (c), (d) phase, (e), (f) in-phase images. The arrows point along the polarization directions. The scans size is $5 \times 5 \mu\text{m}^2$.

with the brown one standing for zero PR. These scans clearly reveal the presence of domain walls (zero OP-PR stripes in figure 4a), as well as large areas with zero IP-PR (figure 4b). The latter corresponds to domains with the IP polarization component either parallel or antiparallel with the cantilever, that is, along two co-linear $\langle 110 \rangle$ directions.

The phase images (figures 4c and d) provide a great deal of information about the direction of polarization in domains, but scans along different crystallographic directions are necessary to reconstruct the vector direction. The dominant dark tone in the OP phase image in figure 4c stands for a phase value of $+170^\circ$, while the white tone represents a phase value of -10° . Thus, the two domains are 180° apart in phase with the dominant one pointing down as proven by performing poling experiments (see below). The white domains in the IP phase image (figure 4d) stand for a phase of -20° . In the noisy domains, the phase signal fluctuates between -180° and $+180^\circ$ due to the lack of PR signal. This is in agreement with the observation of zero-amplitude domains in figure 4b. By rotating the sample, for example 180° , dark phase domains standing for a phase of $+160^\circ$ have been seen as well, because of the $\langle 111 \rangle$ orientation of polarization. The in-phase images (figures 4e and f) contain all the information obtained from the corresponding amplitude and phase images and are, therefore, sufficient for the study of ferroelectric domain structure and domain dynamics, as we show below. For the film illustrated in figure 4, two down polarization domains separated by a 71° ferroelastic domain wall [14, 15] fully describe the observed pattern (see the arrows in figures 4b-f).

The stripe domain structure contains only two of eight possible polarization variants. The two polarization variants in the stripe pattern belong to two distinct structural variants with the domain walls running along the pseudocubic $\langle 100 \rangle$ direction. Such a domain structure was observed earlier in (001)-oriented epitaxial $\text{PbZr}_{0.80}\text{Ti}_{0.20}\text{O}_3$ and $\text{PbZr}_{0.65}\text{Ti}_{0.35}\text{O}_3$ films and was seen as a consequence of mechanical and charge compatibility conditions [37]. It was recently found both theoretically, by performing phase-field simulations [46], and experimentally, by reducing the growth rate of the underlying SrRuO_3 layer, that a similar domain structure forms in thin epitaxial BiFeO_3 films as well [47]. At low deposition rates, the growth mode changes from step-bunching to step-flow [48] and a single domain epitaxial SrRuO_3 underlayer forms, which promotes the growth of stripe domain BiFeO_3 epitaxial films [47].

Following the same procedure as above, one can identify all electric field-induced polarization switching mechanisms in epitaxial BiFeO_3 films. To locally switch the films, a dc bias was applied to the conducting AFM probe while scanning over the desired area. The poled area is conspicuous in the OP image (figure 5a), confirming film switching. We note that the images in figure 5 were taken in the same area as those shown in figure 4. While the interpretation of OP image is straightforward, the colour changes in IP scans correspond in general to several types of switching processes, namely 180° , 109° and 71° [15]. For the sake of simplicity, we show a simple IP contrast change in figure 5b, which corresponds to a dominant 180° polarization switching (see the arrows in figures 5b and c). Along with this image we show the initial IP domain structure in figure 5c. In this way, one can easily see that aside from the colour change in the poled area, the overall pattern in figure 5c does not exactly match the one in figure 5b due to ferroelastic switching.

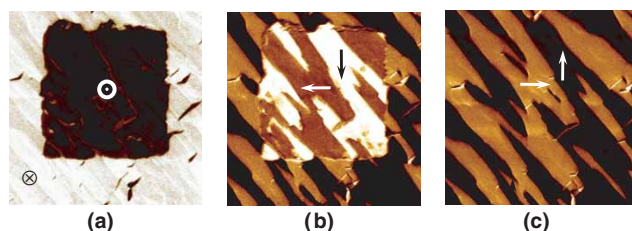


Figure 5. Switching of ferroelectric polarization in an epitaxial BiFeO_3 film imaged by in-phase PFM. The images were taken in the same area as those in figure 4. (a) Out-of-plane and (b) in-plane PFM scans taken after electrical poling. (c) Corresponding in-plane PFM scan taken before poling. The arrows point along the polarization directions. The scans size is $5 \times 5 \mu\text{m}^2$.

By analyzing the IP contrast change following electrical poling in epitaxial BiFeO_3 (001) films, all three possible switching mechanisms have been observed [15].

5. Some future directions

5.1. Decreasing the coercive field of BiFeO_3

Significant progress has been recently demonstrated on the integration of BiFeO_3 on Si(001) substrates by using a SrTiO_3 template layer with a SrRuO_3 bottom electrode [13]. However, the epitaxial BiFeO_3 films grown on Si(001) show coercive fields of 200 kV/cm and a large leakage level, which block their pathway to device applications. Lowering the coercive field to below 100 kV/cm as well as reducing leakage have, thus, become critical issues.

To achieve these aims, one could, for instance, follow the La-substitution procedure at the A^{3+} -site as in the case of tetragonal $\text{PbZr}_x\text{Ti}_{1-x}\text{O}_3$ [49, 50]. Rare-earth substitutions at the Bi^{3+} site have been attempted in the past [51]. For instance, it was found that in La-substituted BiFeO_3 , both the ferroelectric Curie temperature and lattice constant decrease with increasing La concentration [52, 53]. Most recently, it has been reported that La-substitution at the Bi site improves the electrical properties of BiFeO_3 to some extent [54–56], but no insights on the actual role of dopant has been given. Therefore, further efforts have to be directed on understanding the mechanisms responsible for the large coercive fields and leakage currents.

5.2. Ferroelectric-antiferromagnetic coupling in BiFeO_3

BiFeO_3 has the remarkable property of simultaneously being a very good ferroelectric and antiferromagnetic at room temperature. Naturally, the question of whether there is any coupling between the corresponding order parameters arises, although a ferroelectric-induced spin canting mechanism as in BaFMn_4 [27, 28] is forbidden for symmetry reasons. However, a domain wall magnetoelectric coupling

mechanism [57] is allowed in epitaxial BiFeO_3 films. In an atomistic picture, the antiferromagnetic easy plane is determined by the relative orientation between the Fe cation and oxygen octahedra. Polarization rotation results in a modification of the oxygen configuration around the shifting Fe cation. This might affect the superexchange interaction between the Fe cations, which in turn alters the local magnetic order. Undoubtedly, the technological potential of a room temperature electrically tunable antiferromagnet is huge. Despite this, only a few experimental and theoretical works aimed at elucidating this aspect [12, 18, 24, 29], mainly due to the difficulty in discriminating between the ferroelectric and magnetic contributions.

Just recently, using PFM and photoemission electron microscopy (PEEM) with linearly polarized X-ray, a strong correlation between the ferroelectric and antiferromagnetic domain structures of an epitaxial BiFeO_3 film was observed by Zhao *et al.* [29]. By analyzing the local changes in the ferroelectric and antiferromagnetic domain structures following the application of an electrical bias, it was shown that ferroelastic switching leads to a reorientation of the antiferromagnetic easy plane [29]. An aspect that we are currently looking into is the role of epitaxial constraint on the nature of antiferromagnetism: it is quite possible that epitaxial strain can change the (111) easy plane of magnetization into an easy axis (possibly of the [110] or [112] type). Furthermore, the nature of magnetism at the ferroelastic domain walls [14, 15] (71° and 109° , with the additional possibility of both head-to-head and head-to-tail orientations) needs to be carefully understood. The importance of understanding the polarization switching in thin epitaxial BiFeO_3 films is two-fold. First, this enables the possibility of tuning the ferroelectric properties by domain engineering. Second, the direct observation of polarization rotation opens the exciting opportunity to investigate the coupling between the ferroelectric and antiferromagnetic order parameters at room temperature. Significant effort is currently aimed at addressing these two issues and the most recent results are meeting the expectations.

5.3. Ferroelectric-ferromagnetic coupling through the multiferroic BiFeO_3

By far the most exciting area of research involving such multiferroic materials systems is the potential to electrically control magnetism!! There is feverish work on-going around the world aimed at solving this problem. One possible materials heterostructure is described schematically in figure 6. This consists of an antiferromagnetic-ferroelectric (i.e. the multiferroic) in contact with a conventional ferromagnet. For instance, epitaxial $\text{BiFeO}_3/\text{La}_{2/3}\text{Sr}_{1/3}\text{MnO}_3$ heterostructures have been grown on $\text{SrTiO}_3(001)$ [58] without suppressing the ferroelectric order in BiFeO_3 [59]. In the absence of ferroelectricity in the multiferroic, such heterostructure would correspond to the classical ‘exchange bias’ structure. Indeed, sizeable tunnelling magnetoresistance and exchange bias effects have been reported on epitaxial $\text{BiFeO}_3/\text{La}_{2/3}\text{Sr}_{1/3}\text{MnO}_3$ and $\text{BiFeO}_3/\text{CoFeB}$ -based heterostructures [60]. However, by introducing the multiferroicity in the antiferromagnet, we now have the potential to electrically control the state of the antiferromagnet and, thereby, indirectly control the state of the ferromagnet. Preliminary work in this direction

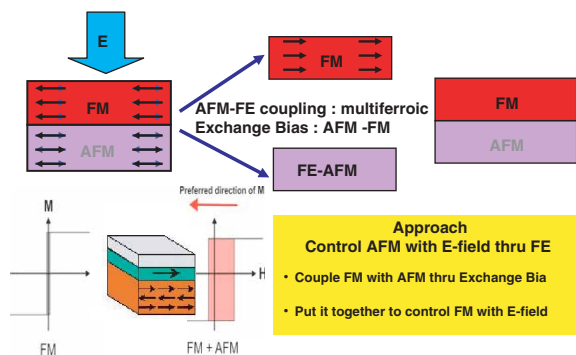


Figure 6. Sketch of a possible heterostructure to achieve the electrical control of magnetism through the multiferroic BiFeO_3 .

shows considerable promise; clearly a lot of our research effort will remain focused on this exciting possibility.

Acknowledgments

The authors would like to thank R. R. Das, D. M. Kim, S. H. Baek, P. Shafer, A. Scholl, J. X. Zhang, C. Ederer, N. A. Spaldin, L. Q. Chen, C. B. Eom and D. G. Schlom for their invaluable contributions. This work has been supported by the Director, Office of Basic Energy Sciences, Materials Sciences Division of the US Department of Energy under contract DE-AC02-05CH11231 and an ONR-MURI grant No. E-21-6RU-G4. The authors acknowledge support of the National Center for Electron Microscopy, Lawrence Berkeley Laboratory.

References

- [1] Van E. Wood and A.E. Austin, *Intl. J. Magn.* **5** 303 (1974).
- [2] L.D. Landau and E.M. Lifshitz, *Electrodynamics of Continuous Media* (Addison-Wesley/Pergamon Press, Oxford, 1960), p. 119.
- [3] M. Fiebig, *J. Phys. D* **38** R123 (2005).
- [4] N.A. Spaldin and M. Fiebig, *Science* **309** 391 (2005).
- [5] W. Eerenstein, N.D. Mathur and J.F. Scott, *Nature* **442** 759 (2006).
- [6] N.A. Hill, *J. Phys. Chem. B* **104** 6694 (2000).
- [7] M. Fiebig, Th. Lottermoser, D. Fröhlich, *et al.*, *Nature* **419** 818 (2002).
- [8] Th. Lottermoser, Th. Lonkai, U. Amann, *et al.*, *Nature* **430** 541 (2004).
- [9] T. Kimura, T. Goto, H. Shintani, *et al.*, *Nature* **426** 55 (2003).
- [10] S. Dong, J.F. Li and D. Viehland, *Phil. Mag. Lett.* **83** 769 (2003).
- [11] S. Shastry, G. Srinivasan, M.I. Bichurin, *et al.*, *Phys. Rev. B* **70** 064416 (2004).

- [12] J. Wang, J.B. Neaton, H. Zheng, *et al.*, *Science* **299** 1719 (2003).
- [13] J. Li, J. Wang, M. Wuttig, *et al.*, *Appl. Phys. Lett.* **84** 5261 (2004).
- [14] F. Zavaliche, R.R. Das, D.M. Kim, *et al.*, *Appl. Phys. Lett.* **87** 182912 (2005).
- [15] F. Zavaliche, P. Shafer, M.P. Cruz, *et al.*, *Appl. Phys. Lett.* **87** 252902 (2005).
- [16] R.R. Das, D.M. Kim, S.H. Baek, *et al.*, *Appl. Phys. Lett.* **88** 242904 (2006).
- [17] J.R. Teague, R. Gerson and W.J. James, *Solid State Commun.* **8** 1073 (1970).
- [18] C. Ederer and N.A. Spaldin, *Phys. Rev. B* **71** 060401(R) (2005).
- [19] C. Ederer and N.A. Spaldin, *Phys. Rev. B* **71** 224103 (2005).
- [20] J.B. Neaton, C. Ederer, U.V. Waghmare, *et al.*, *Phys. Rev. B* **71** 014113 (2005).
- [21] C. Ederer and N.A. Spaldin, *Phys. Rev. Lett.* **95** 257601 (2005).
- [22] Lebeugle *et al.*, in Conference sur Multiferroique, Gif Sur Yvette, France, November (2006).
- [23] G.A. Smolenskii and I. Chupis, *Sov. Phys. Usp.* **25** 475 (1982).
- [24] P. Baettig, C. Ederer and N.A. Spaldin, *Phys. Rev B* **72** 214105 (2005).
- [25] G.A. Samara and P.M. Richards, *Phys. Rev. B* **14** 5073 (1976).
- [26] G.A. Samara and J.F. Scott, *Solid State Commun.* **21** 167 (1977).
- [27] D.L. Fox and J.F. Scott, *J. Phys. C* **10** L329 (1977).
- [28] D.L. Fox, D.R. Tilley, J.F. Scott, *et al.*, *Phys. Rev. B* **21** 2926 (1980).
- [29] T. Zhao, A. Scholl, F. Zavaliche, *et al.*, *Nat. Mater.* **5** 823 (2006).
- [30] Y.W. Li, J.L. Sun, J. Chen, *et al.*, *Appl. Phys. Lett.* **87** 182902 (2005).
- [31] X. Qi, J. Dho, M. Blamire, *et al.*, *J. Magn. Magn. Mater.* **283** 415 (2004).
- [32] W. Eerenstein, F.D. Morrison, J. Dho, *et al.*, *Science* **307** 1203a (2005).
- [33] J. Wang, A. Scholl, H. Zheng, *et al.*, *Science* **307** 1203b (2005).
- [34] C. Michel, J.-M. Moreau, G.D. Achenbechi, *et al.*, *Solid State Commun.* **7** 701 (1969).
- [35] F. Kubel and H. Schmid, *Acta Crystallogr. B* **46** 698 (1990).
- [36] M. Abplanalp, D. Barošová, P. Bridenbaugh, *et al.*, *J. Appl. Phys.* **91** 3797 (2002).
- [37] S.K. Streiffer, C.B. Parker, A.E. Romanov, *et al.*, *J. Appl. Phys* **83** 2742 (1998).
- [38] A.E. Romanov, M.J. Lefevre, J.S. Speck, *et al.*, *J. Appl. Phys* **83** 2754 (1998).
- [39] Y.L. Li, S.Y. Hu and L.Q. Chen, *J. Appl. Phys.* **97** 034112 (2005).
- [40] P. Güthner and K. Dransfeld, *Appl. Phys. Lett.* **61** 1137 (1992).
- [41] A. Gruverman, O. Auciello and H. Tokumoto, *Annu. Rev. Mater. Sci.* **28** 101 (1998).
- [42] S.V. Kalinin and D.A. Bonnell, *Phys. Rev. B* **65** 125408 (2002).
- [43] H. Koizumi, N. Niizeky and T. Ikeda, *Jpn. J. Appl. Phys.* **3** 495 (1964).
- [44] C.B. Eom, R.J. Cava, R.M. Fleming, *et al.*, *Science* **258** 1766 (1992).
- [45] C.S. Ganpule, V. Nagarajan, B.K. Hill, *et al.*, *J. Appl. Phys.* **91** 1477 (2002).
- [46] L.Q. Chen, *Annu. Rev. Mater. Res.* **32** 113 (2002).
- [47] Y.H. Chu, Q. Zhan, L.W. Martin, *et al.*, *Adv. Mater.* **18** 2307 (2006).
- [48] W. Hong, H.N. Lee, M. Yoon, *et al.*, *Phys. Rev. Lett.* **95** 095501 (2005).
- [49] B. Yang, T.K. Song, S. Aggarwal, *et al.*, *Appl. Phys. Lett.* **71** 3578 (1997).
- [50] T.K. Song, S. Aggarwal, A.S. Prakash, *et al.*, *Appl. Phys. Lett.* **71** 2211 (1997).
- [51] Z.V. Gabbasova, M.D. Kuz'min, A.K. Zvezdin, *et al.*, *Phys. Lett. A* **158** 491 (1991).
- [52] M. Polomska, W. Kaczmarek and Z. Pajak, *Phys. Stat. Sol.* **23** 567 (1974).
- [53] Yu.E. Roginskaya, Yu.N. Venetsev, S.A. Fedulov, *et al.*, *Sov. Phys. Crystallogr.* **8** 490 (1964).
- [54] H. Uchida, R. Ueno, H. Nakaki, *et al.*, *Jpn. J. Appl. Phys.* **44** L561 (2005).
- [55] D. Lee, M.G. Kim, S. Ryu, *et al.*, *Appl. Phys. Lett.* **86** 222903 (2005).
- [56] Y.-H. Lee, J.-M. Wu and C.-H. Lai, *Appl. Phys. Lett.* **88** 042903 (2006).
- [57] J. Privratska and V. Janovec, *Ferroelectrics* **204** 321 (1997).
- [58] H. Béa, M. Bibes, M. Sirena, *et al.*, *Appl. Phys. Lett.* **88** 062502 (2006).
- [59] H. Béa, S. Fusil, K. Bouzehouane, *et al.*, *Jpn. J. Appl. Phys.* **45** L187 (2006).
- [60] H. Béa, M. Bibes, S. Cherifi, *et al.*, *Appl. Phys. Lett.* **89** 242114 (2006).